Excitons in large-gap insulators: Solid neon*

W. Andreoni
Istituto di Fisica, Università di Roma, Roma, Italy
and Centre Européen de Calcul Atomique et Moléculaire, Bâtiment 506, Université de Paris XI, Orsay, France

F. Perrot
Commissariat à l'Energie Atomique, Centre d'Etudes de Limeil, Boîte Postale No. 27, 94 Villeneuve St Georges, France

F. Bassani
Istituto di Fisica, Università di Roma, Roma, Italy
(Received 12 April 1976)

Excitons at the fundamental edge ($17 < E < 22$ eV) of solid neon are studied. The lowest transverse and longitudinal states ($n = 1$) are determined in the framework of the integral-equation approach assuming that the electron and the hole be confined to the same unit cell (one-site approximation). Numerical calculations are performed according to the general scheme previously applied successfully to valence and core excitons in solid argon. The lowest-conduction-band structure has been fully accounted for, using a detailed augmented-plane-wave calculation. Good agreement with the experimental results has been obtained. Higher excitons ($n > 1$) are determined in the effective-mass approximation, modified to include the spin-orbit splitting of the valence band and the electron-hole exchange interaction, the latter being estimated from the excitation spectrum of gaseous neon. Full correspondence of the atomic transitions $(2p)^6 \rightarrow 2p^5ms$ ($m \geq 3$) and $n \geq 1$ valence excitons in solid neon has been established. Relative intensities of the partners in the nth doublets ($n \geq 1$) are determined explaining the presence of only one exciton series in solid neon, unlike other rare-gas solids. Further structure above the threshold has been interpreted in terms of the joint density of states.

I. INTRODUCTION

The optical spectra of the solid rare gases[1] corresponding to the electronic transitions from the valence states have been studied for several years by using conventional radiation sources.[2] During the past few years, the use of synchrotron radiation as a continuum source has allowed us to extend the energy range of interest over about 500 eV,[3] as well as to investigate in detail the fine structure at the fundamental edge of the interband transitions.[4] Recently, also radiationless electronic energy-transfer processes have been studied using photoemission yield spectroscopy, on pure[5] as well as on doped[6] solid rare gases. In addition, electron-energy-loss measurements have been performed.[7] Further information about the electronic structure of the solid rare gases has been provided by photoelectron energy distribution data.[8]

From the above experiments detailed exciton spectra have been resolved at the onset of interband transitions; in particular two Rydberg series have been resolved in Ar, Kr, and Xe but only one series in solid neon. The main problems which arise in the interpretation of the excitation spectra of solid rare gases are the following: (a) an adequate description of the lowest ($n = 1$) exciton states; they cannot be understood in the Frenkel-Peierls model nor in the Wannier-Mott scheme[1,9,10]; (b) the relative contribution of the spin-orbit interaction and of the electron-hole (e-h) exchange interaction in determining the relative oscillator strengths of the partners in the doublet structure; (c) the position of the edge and the energy sequence of the $n > 1$ excitons; (d) the interpretation of the structure above the edge.

In a previous paper,[10] which we shall refer to as I from now on, we have studied the $n = 1$ excitons in solid argon and we have obtained a very good agreement with the experimental results. We have performed the calculations in the integral-equation approach,[11] which is based on the use of Wannier functions to express the electron and the hole wave functions and of the Green's functions relative to the conduction and valence bands to give the contribution of the band structure on the entire Brillouin zone (BZ).

It is the purpose of the present paper to apply the same theory to the valence excitons in solid neon, where the contributions of the spin-orbit interaction of the hole states and of the e-h exchange interaction must be carefully assessed, the former being smaller than the short-range exchange term.

Previous descriptions[12,13] of the $n = 1$ exciton in the effective-mass approximation (EMA) have shown a displacement from its position in the Rydberg series by more than 1 eV, requiring a large central cell correction. Another description

has been attempted by Webber, Rice, and Jortner[14] with an expansion in excited atomic states delocalized over many lattice cells. This is essentially the Frenkel-Peierls model with the modification that the excited wave functions centered on different cells be orthogonal. The results are inconclusive owing to the fact that the atomic excited wave functions, though properly orthonormalized in the crystal, are not suitable approximations to the corresponding Wannier functions in cases like neon.[15] In addition, the disappearance of the spin-orbit partners in the lowest excitons of neon has been misunderstood so far,[16] being ascribed to an experimental broadening of the peak, and no attempt has been made to understand the $n>1$ excitons.

In the present paper we give a numerical calculation of the lowest ($n=1$) excitons performed with the integral-equation method. We also compute the higher-exciton states by modifying the EMA approach of Onodera and Toyozawa[17] to take a better account of the e-h exchange. We also give a quantitative account for the continuum spectrum above threshold based on the joint-density of states of the valence and the conduction bands with a plasmon contribution.[18]

In Sec. II we give a general mathematical formulation appropriate to the excitation spectrum of solid rare gases. In Sec. III we present the calculation of the relevant parameters from the band structure of solid neon. In Sec. IV we give the results and compare them to experimental data. In Sec. V we give our conclusions.

II. MATHEMATICAL APPROACH TO EXCITON STATES IN SOLID RARE GASES

We must consider separately the lowest-exciton states ($n=1$) and the higher-exciton states ($n>1$). In the former case the exciton wave function is essentially confined in the unit cell and we may use the intermediate binding approach of I and adopt the one-site approximation. In the latter case the exciton wave functions extend over a number of cells and calculations are much more complicated. For $n\gg1$ the integral equation appropriate to the intermediate binding regime reduces to the differential equation of the EMA and the exciton levels are given by a Rydberg series.[19] We adopt this approach for all the $n>1$ states, with suitable modifications of the exchange contribution for the low values of n.

The optical transitions which are relevant to the excitation spectrum of solid neon between 17 and 30 eV are those associated with the valence states corresponding to the $2p$ states in the atom and the first conduction states corresponding to the $3s$ excited ones. In the crystal the valence band can be essentially understood in the tight-binding scheme and consists of three branches with a small $\vec{k}$ dependence (bandwidth $\Delta E_v \simeq 0.2$ eV) and a small spin-orbit splitting at $\vec{k}=0$ ($\Delta \simeq 0.09$ eV), while the conduction band is a simple s-like band, separated from higher d-like and p-like conduction bands, and nearly-free-electron-like (bandwidth $\Delta E_c = 7.40$ eV).

In Fig. 1 we plot the energy bands in solid neon, as computed in a modified augmented-plane-wave method described by Dagens and Perrot.[20] The approach consists essentially in adopting a spherical atomic-like Hartree-Fock exchange operator and a muffin-tin Coulomb potential in the framework of the augmented-plane-wave method. Polarization effects are also taken into account both for the conduction electrons[21] and for the valence states, resulting in a correlation correction of -1.57 eV for the conduction electron at $\vec{K}=0$ and a mean correction of about 2.43 eV for the valence states at $\vec{K}=0$. Relativistic effects are estimated in a perturbative way: the spin-orbit separation of the valence band $\Delta(\vec{k})$ has been computed in first order in the tight-binding approach by using for the valence Bloch functions appropriate combinations of $2p$ orbitals,[22] and expressing the matrix elements of the spin-orbit operator in terms of

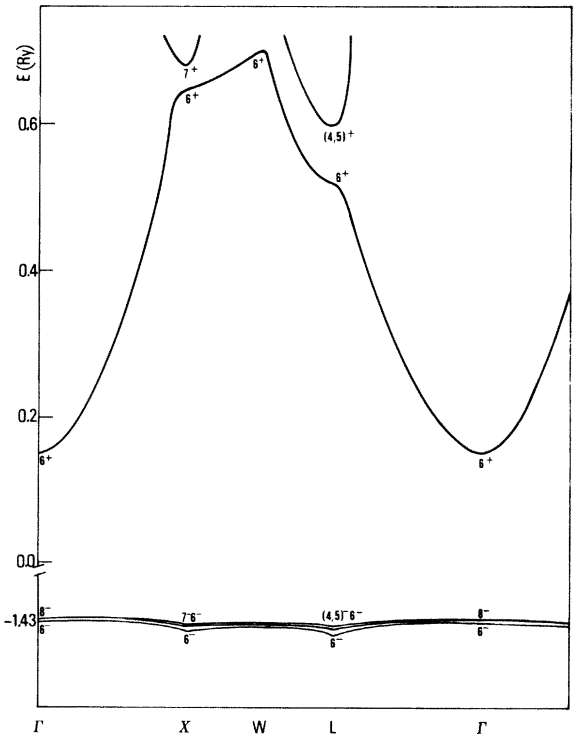

FIG. 1. Energy bands of solid neon.

the atomic splitting ξ.[23] For instance, at the center Γ of the BZ, we use the following expressions:

$$E(\Gamma_{8^-}) = E_0 + \xi/3O(pp) \tag{1a}$$

and

$$E(\Gamma_{6^-}) = E_0 - 2\xi/3O(pp), \tag{1b}$$

where $O(pp)$ is the normalization of the Bloch function at $\vec{K}=0$, which is smaller than one for p-like functions.

In the following we will neglect higher conduction bands and will take the two spin-orbit split valence bands as independent of $\vec{k}$, which is a very good approximation because of the small width of the valence band. The Fredholm solutions of the integral equation for the two lowest Γ_{15} excitons in the one-site approximation can be obtained as the zeros of the determinant[10]

$$\begin{vmatrix} 1+[\frac{4}{3}(J+D)-Q]G_{8^-}(E) & -\frac{2}{3}\sqrt{2}\,(J+D)G_{8^-}(E) \\ -\frac{2}{3}\sqrt{2}(J+D)G_{6^-}(E) & 1+[\frac{2}{3}(J+D)-Q]G_{6^-}(E) \end{vmatrix}. \tag{2}$$

In the above expression Q and J are Coulomb and exchange integrals between electron and hole Wannier functions located on the same cell and D is the long-range exchange term which is different for transverse and longitudinal excitons; namely,

$$D_t = -(4\pi/3\epsilon_0)n_0\mu_x^2, \tag{3a}$$

$$D_l = (8\pi/3\epsilon_0)n_0\mu_x^2, \tag{3b}$$

with $\epsilon_0 = 1.26$ for solid neon. We consider screening effects negligible in the short-range interaction terms and described by the static dielectric constant ϵ_0 in the long-range interaction terms, according to the discussion developed in I for the similar case of the solid argon. The Green's functions $G_{8^-}(E)$ and $G_{6^-}(E)$ are given by

$$G_{8^-}(E) = N^{-1}\sum_{\vec{k}\in BZ}[E_{\Gamma_{6^+}}(\vec{k}) - E_{\Gamma_{8^-}}(\vec{k}) - E]^{-1} \tag{4}$$

with a similar expression for $G_{6^-}(E)$ referred to the split-off valence band. (We have labeled the energy bands with their symmetry at $\vec{K}=0$.)

The diagonal terms in Eq. (2) give two exciton states, each associated to one of the two valence bands separated by the spin-orbit interaction [in our approximation $\Delta(\vec{k}) \approx \Delta(\vec{K}=0) \equiv \Delta$], while the off-diagonal terms represent their admixture induced by e-h exchange. Inserting D_t or D_l in Eq. (2) we obtain transverse and longitudinal excitons, respectively. The relative transition probabilities for two eigenstates associated to the valence edges Γ_{8^-} and Γ_{6^-} take the values 2 : 1 when the off-diagonal term in Eq. (2) can be neglected, which turns out to be the case when exchange is much smaller than Δ. Otherwise they can be computed from the solutions of Eq. (2) as indicated in I.

The $n>1$ excitons may be represented in the EMA as suggested by Onodera and Toyozawa[17]; however, we must introduce modifications to account for excitons with small values of n. In fact in solid neon the exchange cannot be included in the EMA as a δ-function potential because the Bohr radius extends over a few neighboring cells where exchange is not yet negligible. Therefore we choose to adopt the EMA without exchange and spin-orbit interactions to give zero-order solutions which can be classified according to their total spins. The exchange operator splits triplet and singlet states and the spin-orbit operator mixes them by an amount which depends only on the ratio $\eta_n \equiv 2(J_n+D_n)/\Delta$. The wave functions in the presence of both perturbations are

$$\Psi_{n,\Gamma_{15}}(r_e, r_h) = a\Phi^{s=0}_{n,\Gamma_{15}}(r_e, r_h) + b\Phi^{s=1}_{n,\Gamma_{15}}(r_e, r_h), \tag{5}$$

where any of the exciton functions with definite spin can be considered in the two-particle representation[24] as the product of an envelope function $F_n(\vec{r}_e - \vec{r}_h)$ by the properly symmetrized electron and hole functions at the band edges. The coefficients a and b give the singlet-triplet mixing and are determined from the following eigenvalue equation:

$$\begin{vmatrix} E_n^0 + 2(J_n+D_n) - E_n & (-\sqrt{2}/3)\Delta \\ (-\sqrt{2}/3)\Delta & E_n^0 + \frac{1}{3}\Delta - E_n \end{vmatrix} = 0, \tag{6}$$

and the corresponding linear equations. The exchange contribution consists of two terms which depend on the quantum number n in a different way. J_n is the e-h exchange term which depends on the size of the envelope function and D_n is the screened dipole-dipole interaction which depends on the value of the envelope function at $r=0$ and is related to Eq. (3) by

$$D_n = D|F_n(0)|^2. \tag{7}$$

From the solutions of Eq. (6) one can obtain the splitting between the two excitons and their relative intensities. When the energies are measured in units of the spin-orbit splitting Δ, the exciton separation $\delta E_n = (E_1 - E_2)_n$ and the intensity ratio of the doublet can be expressed as universal functions of $\eta_n = 2(J_n+D_n)/\Delta$; namely, as

$$\delta E_n = |1 - \tfrac{2}{3}\eta_n + \eta_n^2|^{1/2}, \tag{8}$$

$$\rho_n = (I_1/I_2)_n = \tfrac{8}{9}(\eta_n + \delta E_n - \tfrac{1}{3})^{-2}. \tag{9}$$

III. CALCULATION OF GREEN'S FUNCTIONS, WANNIER FUNCTIONS, AND MATRIX ELEMENTS FOR SOLID NEON

In order to evaluate the parameters Q, J, and D entering Eq. (2), we need to compute the Wannier functions of the valence and conduction bands as shown in I.

The Wannier functions relative to the valence bands are taken to coincide with the $2p$ atomic functions of neon, as obtained analytically by Bagus,[22] because the overlap between neighboring sites is practically negligible. The Wannier function of the lowest conduction band has been computed from Bloch functions constructed as single plane waves orthogonalized to the core and valence occupied states expressed as appropriate Bloch lattice sums. We follow the same procedure as in I and obtain a Wannier function which is more localized than the excited atomic $3s$ function.[25] In Fig. 2 we display the Wannier function $a(\vec{r})$ obtained in this way in the direction of the nearest neighbors, [110], and in Fig. 3 we compare its spherical part $a_0(r)$ to the $3s$ orbital.

The Wannier function $a(\vec{r})$ has been expanded in cubic harmonics and the relevant integrals have been computed. Their values are given in Table I and in Table II. The results of Table I indicate a good convergence with values up to $l=10$ in the spherical-harmonic expansion. The value of Δ in Table II has been computed from Eq. (1) where the atomic spin-orbit splitting is taken to be $\xi = 0.0967$ eV,[23] and the overlap integrals have been evaluated to be $S(pp\sigma) = -0.0085$ and $S(pp\pi) = 0.0012$.

The Green's functions have been computed from the detailed energy-band calculations giving the band structure displayed in Fig. 1. Expression (4) is numerically computed from the density of states $n(E')$

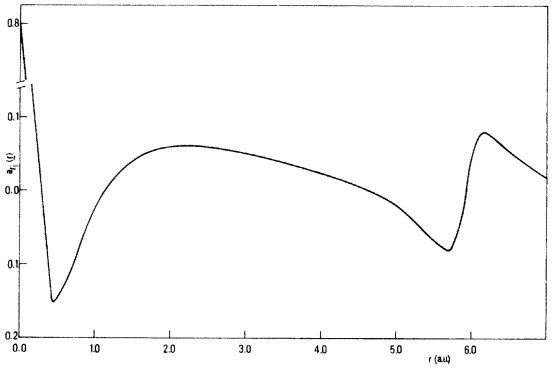

FIG. 2. Wannier function $a(\vec{r})$ relative to the lowest neon conduction band along the [110] direction.

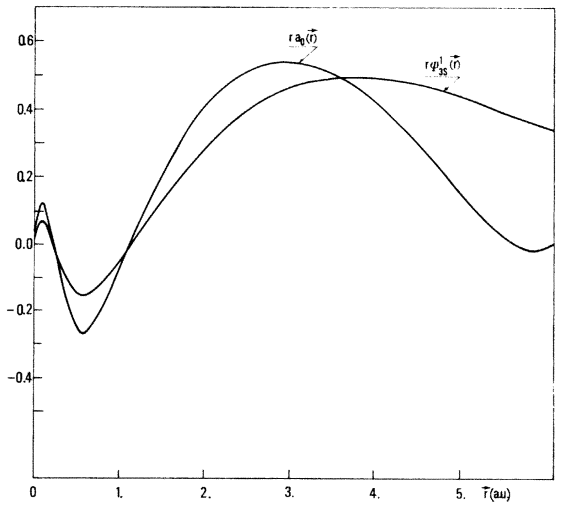

FIG. 3. Spherical contribution to the Wannier function $ra_0(\vec{r})$ compared with the $3s$ atomic neon function $r\psi_{3s}(\vec{r})$, as computed by Gold and Knox in Ref. 25.

$$G_{8^-}(E) = \int_0^{E_m} n(E')[E' + E_g(\Gamma_{8^-}) - E]^{-1} dE' , \quad (10)$$

with an analogous expression for $G_{6^-}(E)$. The density of states $n(E')$ has been computed by numerical integration with a Monte Carlo method from a random choice of 64 000 points in the BZ, the energy bands being interpolated from the value computed at 89 nonequivalent points in the reduced zone.[26] In this case it turned out to be very important to perform a detailed analysis of the band structure because the conduction band is very wide and a tight-binding interpolation, as that used in solid argon, would not have been suitable. In Fig. 4 we report the Green's function $G_{8^-}(E)$ for solid neon.

For the higher excitons ($n>1$) we must compute the values of J_n, D_n in addition to the unperturbed energy values. The latter have been calculated from the hydrogenlike equation with an effective Rydberg of 6.85 eV, corresponding to a dielectric function $\epsilon_0 = 1.26$ and to an exciton reduced mass

TABLE I. Coulomb and exchange integrals for solid neon. Contributions from the different angular momentum components to Coulomb and exchange interaction terms are given. $n_0\mu_x^2$ gives the dipolar sums D_t and D_l. Values are in eV.

	1	0	4	6	8	10	Total
Q		7.696	0.136	0.151	0.058	0.002	8.043
J		0.236	2×10^{-5}	3×10^{-5}	8×10^{-6}	9×10^{-9}	0.236
$n_0\mu_x^2$							0.010

TABLE II. Parameters for $n=1$ excitons in solid neon. Calculated values (in eV) of the parameters to be used for $n=1$ excitons [Eq. (2)].

Q	J	D_t	D_1	Δ
8.043	0.236	−0.042	0.084	0.10

$\mu_{exc}=0.8m_e$.[27] The parameters are given in Table III for $n=2-5$. The value D_n is computed from Eq. (7) and turns out to be negligible while J_n is estimated from the corresponding atomic value by comparing the exciton series to the successive lines in the atomic excitation spectrum. The atomic excited configuration corresponding to the $n=1$ excitons is $(2p)^5(3s)^1$ and consists of four states, two pure triplets with total angular momentum $J=0$ and $J=2$, and two $J=1$ states which contain both singlet and triplet components.[25] The value of the exchange interaction terms in this configuration have been derived in the atomic case by applying expression (8) with $D_n=0$,[28] from the level splittings which are well known experimentally. By keeping the same ratio between the atomic and the crystal exchange integral (Table II) in the case of the lowest excited state as for the $n>1$ excitons, we can obtain the J_n values, which are given in Table III. The curves which represent the splittings of the two $J=1$ atomic states and their intensity ratios are drawn in Fig. 5 from Eqs. (8) and (9) as functions of the ratio $\eta=2J/\Delta$. The atomic experimental values are indicated in the curve, as well as the corresponding exciton splittings.

IV. THEORETICAL RESULTS AND COMPARISON WITH EXPERIMENTAL DATA

A. $n=1$ excitons in solid neon

In Table IV we report the binding energies of the lowest $n=1$ transverse and longitudinal excitons as obtained from solving Eq. (2) with the parameters given in Table III. We also give the relative contributions $|A_i^{8-}|^2$ and $|A_i^{6-}|^2$, of the two excitation channels associated with a split-off valence band. They turn out to be mixed in a relevant way, because the e-h exchange interaction is predominant over the spin-orbit separation of the hole states. Consequently, the ratio between the intensities of the $n=1$ excitons is completely upset with respect to the value 2 given by the relative degeneracies of the hole states. In fact, the intensity ratio is expressed in terms of the coefficients A_1^{8-} and A_1^{6-} as shown in I, by the expression

TABLE III. Parameters for $n>1$ excitons in solid neon. Values (in eV) of the parameters to be used for higher excitons [Eq. (6)].

n	2	3	4	5
J_n	0.0623	0.0484	0.0219	0.0139
D_n	0	0	0	0

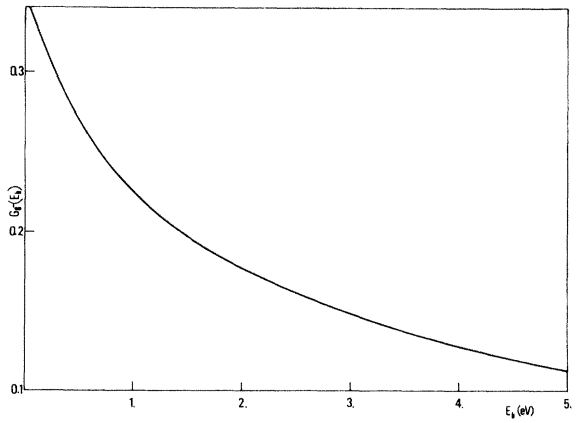

FIG. 4. Green's function $G_{8^-}(E_b)$ as a function of the binding energy $E_b=E_g-E$.

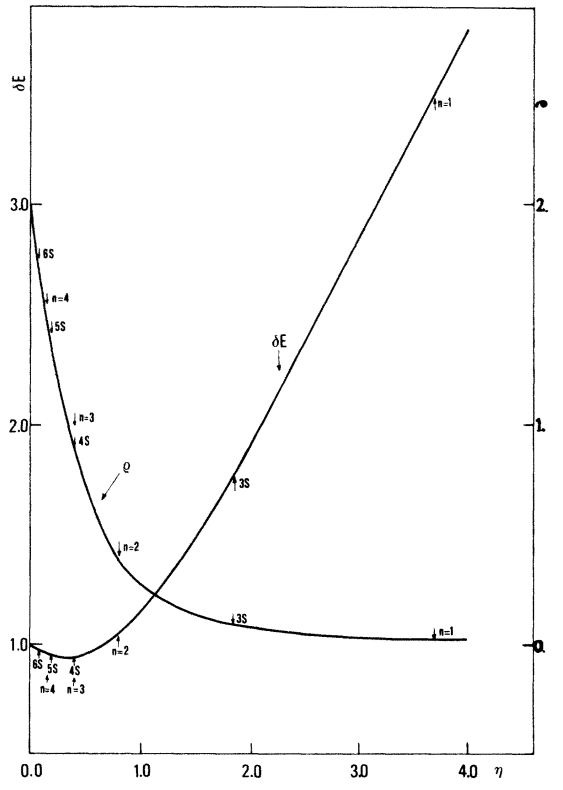

FIG. 5. Separation of the exciton doublet δE_n and intensity ratio $\rho_n=(I_1/I_2)_n$ as a function of $\eta_n=2(J_n+D_n)$ from Eqs. (8) and (9), respectively. Energies are in units of valence-band spin-orbit splitting. Arrows indicate the positions relative to atomic configurations $(2p)^5ms$ to the n excitons.

TABLE IV. Binding energies for the lowest exciton states in solid neon. Theoretical results (in eV) for the binding energies of the $n=1$ transverse and longitudinal excitons are quoted. For comparison, the experimental values obtained in measurements of different kind are given; the latter ones are referred to a band gap of 21.67 eV. The theoretical admixture coefficients $|A_8^-|^2$ and $|A_6^-|^2$ and relative intensities of the two transverse excitons are also given.

	$T_{15}(1,t)$	$T_{15}(2,t)$	$T_{15}(1,l)$	$T_{15}(2,l)$
E_b (th)	4.160	3.814	4.156	3.582
		4.17 [b]		3.92 [e]
E_b (expt)	4.42 [a]	4.27 [c]		3.93 [f]
		4.18 [d]		3.47 [g]
$\|A_8^-\|^2$	0.468	0.532		
$\|A_6^-\|^2$	0.532	0.468		
ρ	1	52		

[a] This value is estimated from the peak observed in the reflectivity spectrum at 17.6 (Ref. 12), assuming the same value for the doublet splitting of the maxima of $\epsilon_2(E)$.

[b] D. Pudewill *et al.* in Ref. 12 (Kramers-Kronig analysis of reflection data).

[c] R. Haensel *et al.* in Ref. 16 (from transmission data).

[d] E. Boursey *et al.* in Ref. 2 (absorption spectrum).

[e] L. Schmidt in Ref. 7 (electron-energy-loss spectrum).

[f] E. J. Daniels and P. Krüger in Ref. 7 (electron-energy-loss spectrum).

[g] G. Keitel, DESY internal report No. F41-70/7 (1970) (Kramers-Kronig analysis of reflectivity data in *c*).

$$\frac{I_1}{I_2} = \frac{1+|A_1^{8-}|^2 - 2\sqrt{2}\, A_1^{8-}A_1^{6-}}{2-|A_2^{8-}|^2 + 2\sqrt{2}\, A_1^{8-}A_1^{6-}} \,. \tag{11}$$

Substituting the values given in Table IV we obtain a ratio of about 1 : 50. For the optically allowed excitons, the ratio of the oscillator strengths of the two partners can also be obtained from the one between the corresponding separations of the longitudinal and transverse modes; namely, as

$$\frac{f_1}{f_2} \approx \frac{(E_l - E_t)_1}{(E_l - E_t)_2} \,. \tag{12}$$

With the values given in Table IV we obtain $f_2/f_1 \simeq 58$, in agreement with the result derived from Eq. (11).

The present results are in fair agreement with experimental data for the lowest excitons. The experimental energy of the strong peak in $\epsilon_2(E)$ at 17.5 eV can be referred to the lowest ionization limit $E_g' = 21.67$ eV, derived in our scheme for the $n>1$ levels, giving a binding energy of 4.17 eV appropriate to the higher level E_2^t. This has to be compared with a computed binding energy of 3.814 eV. The discrepancy is due to the limitation of the one-site approximation. Including the contribution of the nearest cells would decrease the energy and increase the theoretical value of the binding in better agreement with experiment. The contribution of the nearest cells is expected to be more important here than in the case of solid argon since the conduction band is more free-electron-like and the corresponding Wannier function is less localized. It is then natural that the agreement is worse than in the case of argon; however, it is much better than what one would obtain in EMA which gives an effective Rydberg of 6.85 eV. The lowest partner at E_1^t is not usually seen because of its weak oscillator strength. Recent experiments (Ref. 12) have been able to show the position of the lowest-exciton level appearing as a shoulder superimposed to the large higher peak in the reflectivity spectrum, giving a separation of about 0.25 eV.

Energy-loss measurements have been performed in solid neon,[29] giving a strong maximum at 17.75 eV in fair agreement with the computed value of the longitudinal excitons; the theoretical value for the transverse-longitudinal splitting of 0.232 eV compares well with the experimental value of 0.25 eV.

B. $n>1$ excitons and interband transitions in solid neon

For the higher-exciton states we can use the EMA with the corrections given in Sec. III to account for e-h exchange and spin-orbit interaction. We compute two exciton series whose positions and relative intensities are given in Table V. The separations of the doublets practically coincide with the spin-orbit splitting of the valence band and their intensity ratios increase with n to the value 2 : 1. This can be visualized in Fig. 5 in correspondence to the arrows $n=2-5$. The absolute energy positions E_n are obtained from Eq. (6) taking for E_n^0 the EMA result

$$E_n^0 = E_g - R_{\text{eff}}/n^2 \tag{13a}$$

with

$$R_{\text{eff}} = R_H \frac{\mu/m}{\epsilon_0^2} = 6.85 \text{ eV} \,. \tag{13b}$$

The transverse and longitudinal excitons have negligible splittings for $n \geq 2$, so that we do not distinguish between the two.

In Table V we have also given the experimental energy positions of the corresponding atomic excited levels and their relative intensities computed from the graphical analysis of Sec. III. It is interesting to observe that the excitation energies for atomic neon are also given by a Rydberg series for $n>5$, once the correspondences $(2p)^5(3s) \rightarrow n=1$; $(2p)^5(4s) \rightarrow n=2$, and so on, are established. The correspondence between ex-

TABLE V. Higher exciton states in solid neon ($n>1$). Theoretical and experimental excitation energies (in eV) are quoted in the second and third columns, respectively. For comparison, the atomic excited levels are given in the fourth column. Intensity ratios of the doublets in the two cases are quoted in the fifth and sixth columns, respectively. No distinction is made for longitudinal and transverse $n>1$ excitons.

n (m)	E_n (th)	E_n (expt)	ϵ_m (at) [g]	ρ_n (cryst)	ρ_m (at)
2	19.98		19.69		
(4)	20.08	20.31 [a]		0.55	1.19
		20.38 [b]	19.78		
		20.40 [c]			
		20.22 [d]			
		20.30 [e]			
		20.36 [f]			
3	20.93		20.57		
(5)	21.13	20.93 [a]	20.66	0.77	1.34
		21.09 [b]			
		21.10 [c]			
		20.90 [d]			
		20.98 [e]			
		21.0 [f]			
4	21.25		20.94		
(6)		21.35 [a]			
	21.34	21.38 [b]	21.04	1.27	1.67
		21.50 [c]			
		21.25 [d]			
5	21.40		21.15		
(7)	21.50	21.50 [b]	21.24	1.50	1.78
∞	21.67				
			21.56IP		
	21.77		21.66IP		

[a] G. Keitel, internal report No. DESY F41-70/7 (1970) (Kramers-Kronig analysis of reflectivity data in Ref. 16).

[b] D. Pudewill *et al.* in Ref. 12 (minima in transmission spectrum).

[c] R. Haensel *et al.* in Ref. 16 (minima in transmission spectrum).

[d] E. Boursey *et al.* in Ref. 2 (absorption spectrum).

[e] L. Schmidt in Ref. 7 (electron-energy-loss spectrum).

[f] E. J. Daniels and P. Krüger in Ref. 7 (electron-energy-loss spectrum).

[g] C. E. Moore in Ref. 23.

cited configurations in the atom and excitons appears to be well reproduced for the exciton states with s-like envelope function and electron Bloch function of s-like symmetry Γ_1 at $\vec{K}=0$.

We also give in Table V the positions of the exciton peaks in neon as obtained from a number of different experiments. It should be noted that the positions of the $n>1$ levels are not unequivocally established. The failure to observe the doublet splittings, which should be detectable for $n\geq 2$ because of the intensity ratio, can be partly explained as due to the not sufficient resolution and

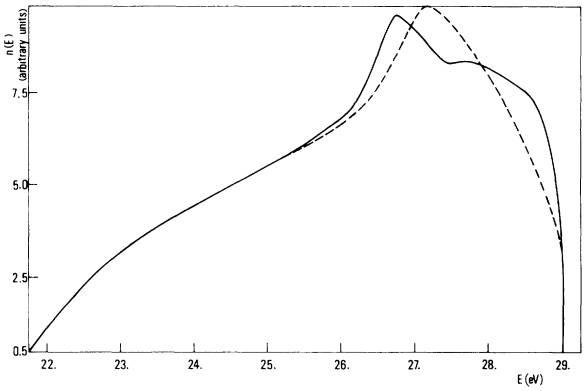

FIG. 6. Joint density of states with (solid line) and without (dashed line) the contribution of the d-like bands in Fig. 1.

to the broadening of the lines. However, careful analysis should display the doublet in the exciton lines and show the two ionization limits, separated by an amount corresponding to the spin-orbit splitting of the valence maxima.

In comparing the theoretical and experimental values of the exciton energies, one can see that the only significant discrepancy occurs for the $n=2$ level. This can be ascribed to the limitation of the effective mass approach which considers the exciton wave function delocalized over many cells in the crystal and therefore tends to overestimate the binding energy.

A further structure in the optical excitation spectrum appears above ionization. This can be related to the density of states of interband transitions which is given in Fig. 6. The peaks occurring in the joint density of states correspond reasonably well to the absorption peaks experimentally observed. In particular a large maximum at about 5.1 eV above ionization corresponds to the transition at the point L, which is a saddle point M_1, as can be seen in Fig. 1. Experimentally, this peak occurs at about 4.4 eV above ionization.[16,28] In the corresponding range of energies, there is a contribution of the second conduction band to the density of states. The position of the theoretical peak could be affected by uncertainties relative to this contribution. A further experimental structure about 7.5 eV above ionization has been interpreted as a plasmon[18] associated with the valence band and would not result in our one-electron picture.

V. CONCLUSIONS

The above calculations confirm the general results obtained in a previous analysis of solid argon and allow a complete interpretation of the optical

spectrum of solid neon. In particular we can summarize the following main conclusions:

(a) Good agreement with the experimental data can be achieved for the lowest excitons with the integral-equation method. No adjustable parameter being involved in our approach, the present results support the validity of the method for calculating intermediately bound excitons.

(b) The lowest exciton structure consists of the doublet separated by exchange and spin-orbit interactions with relative intensities of about 1:50. This strong intensity ratio explains why only one peak is observed.

(c) The large intensity of the observed peak is justified by the large value of its transverse-longitudinal splitting.

(d) The higher exciton peaks ($n > 1$) can be interpreted in the effective mass approximation, including electron-hole exchange and spin-orbit interactions as a perturbation. The triplet-singlet admixture produced by spin-orbit effects tends to make the doublet lines of comparable intensities as the quantum number n increases.

(e) A correspondence can be established between atomic excited configurations $(2p)^5ns$ and the excitons associated to transitions from the valence p-like band to the lowest conduction band, the energy gap corresponding to the ionization atomic energy.

(f) The continuum structure above the edge reflects the structure in the joint density of states but the detailed shape requires consideration of the transition matrix elements and of the electron-hole interaction.

ACKNOWLEDGMENT

One of us (W.A.) wishes to thank Dr. C. Moser, Director of CECAM, for his kind hospitality.

*Based on work performed under the auspices of the CNR through a contract GNSM.

[1]For recent reviews see B. Sonntag and B. Haensel, *Rare gas solids*, edited by M. K. Klein and J. A. Venables (Academic, New York, 1975); U. Rössler, *ibid.*

[2]K. Dressler, J. Quantum Spectrosc. Rad. Transf. 2, 683 (1962); G. Baldini, Phys. Rev. 128, 1562 (1962); J. F. O'Brien and K. J. Teegarden, Phys. Rev. Lett. 17, 919 (1966); I. T. Steinberger and O. Schnepp, Solid State Commun. 5, 417 (1967); I. T. Steinberger, C. Atluri, and O. Schnepp, J. Chem. Phys. 52, 2723 (1970); E. Boursey, J. Y. Roncin, and H. Damany, Phys. Rev. Lett. 25, 1279 (1970); R. Scharber and S. E. Webber, J. Chem. Phys. 55, 3985 (1971).

[3]R. Haensel, G. Keitel, P. Schreiber, and C. Kunz, Phys. Rev. 188, 1375 (1969); Phys. Rev. Lett. 22, 398 (1969); R. Haensel, G. Keitel, C. Kunz, and P. Schreiber, *ibid.* 25, 208 (1970); R. Haensel, G. Keitel, N. Kosuch, U. Nielsen, and P. Schreiber, J. Phys. (Paris) 32, C4-236 (1971); previous measurements in the hard x-ray region have been obtained by J. A. Soules and C. H. Show, Phys. Rev. 113, 470 (1959).

[4]R. Haensel, G. Keitel, E. Koch, M. Skibowski, and P. Schreiber, Phys. Rev. Lett. 23, 1160 (1969); Opt. Commun. 2, 59 (1970); R. Haensel, G. Keitel, E. E. Koch, N. Kosuch, and M. Skibowski, Phys. Rev. Lett. 25, 1281 (1970).

[5]N. Schwentner, M. Skibowski, and W. Steinmann, Phys. Rev. B 38, 2965 (1973); E. E. Koch, V. Saile, N. Schwentner, and N. Skibowski, Chem. Phys. Lett. 28, 562 (1974); I. T. Steinberger, E. Pantos, and I. H. Munro, Phys. Lett. A 47, 299 (1974).

[6]Z. Ophir, B. Raz, J. Jortner, V. Saile, N. Schwentner, E. E. Koch, M. Skibowski, and W. Steinmann, J. Chem. Phys. 62, 650 (1975).

[7]E. M. Hörl and J. A. Suddeth, J. Appl. Phys. 32, 2521 (1961); O. Bostanjoglo and L. Schmidt, Phys. Lett. 22, 130 (1966); P. Keil, Z. Naturforsch. A 21, 503 (1966); Z. Phys. 214, 251 (1968); J. Daniels and P. Krüger, Phys. Status Solidi B 43, 659 (1971); C. Colliex and B. Jouffrey, J. Phys. (Paris) 32, 46 (1971); L. Schmidt, Phys. Lett. A 36, 87 (1971).

[8]N. Schwentner, F. J. Himpsel, E. E. Koch, V. Saile and M. Skibowski, in *Vacuum Ultraviolet Radiation Physics*, edited by E. E. Koch, R. Haensel, and C. Kunz (Pergamon-Vieweg, New York, 1974), p. 335; N. Schwentner, F. J. Himpsel, V. Saile, M. Skibowski, W. Steinmann, and E. E. Koch, Phys. Rev. Lett. 34, 528 (1975); A. B. Kunz, D. J. Mickish, S. K. V. Mirmira, T. Shima, F. J. Himpsel, V. Saile, N. Schwentner, and E. E. Koch, Solid State Commun. 17, 761 (1975).

[9]F. Bassani and G. Pastori-Parravicini, *Electronic States and Optical Transitions in Solids* (Pergamon, New York, 1975), p. 201 ff.; J. Hermanson, Phys. Rev. 150, 660 (1966); U. Rössler, Phys. Status Solidi 42, 345 (1970); U. Rössler and O. Schutz, *ibid.* 56, 483 (1973).

[10]W. Andreoni, M. Altarelli, and F. Bassani, Phys. Rev. B 11, 2352 (1975).

[11]See Ref. 10 and references therein.

[12]D. Pudewill, F. J. Himpsel, W. Saile, N. Schwentner, M. Skibowski, and E. E. Koch, Phys. Status Solidi B (to be published).

[13]U. Rössler in Ref. 9; A. B. Kunz and D. J. Mickish, Phys. Rev. B 8, 779 (1973).

[14]S. Webber, S. A. Rice, and J. Jortner, J. Chem. Phys. 41, 2911 (1964).

[15]U. Rössler, Phys. Status Solidi 42, 345 (1970); L. Dagens and F. Perrot, Phys. Rev. B 5, 641 (1972); A. B. Kunz and D. J. Mickish, in Ref. 13; R. N. Euwema, G. G. Wepfer, G. T. Surratt, and D. L. Wilhite, Phys. Rev. B 9, 5249 (1974).

[16]E. Boursey *et al.* in Ref. 2; R. Haensel, G. Keitel, E. E. Koch, N. Kosuch, and M. Skibowski in Ref. 4.

[17]Y. Onodera and Y. Toyozawa, J. Phys. Soc. Jpn. 22, 833 (1967).

[18]P. V. Giaquinta, E. Tosatti, and M. P. Tosi, Solid State Commun. 19, 123 (1976).

[19]F. Bassani and G. Pastori-Parravicini in Ref. 9,

Chap. 6.
[20]L. Dagens and F. Perrot in Ref. 15.
[21]F. Perrot, J. Phys. (Paris) 33, 929 (1972).
[22]P. S. Bagus, Phys. Rev. A 139, 619 (1965).
[23]C. E. Moore, *Atomic Energy Levels*, Vol. I, circular of the NBS 467 (1949). The atomic spin-orbit splitting of the $2p$ states of the Ne atom is obtained with an excellent resolution from the excitation spectra as 0.0967 eV. Different values are reported in the literature without justification (0.14 eV by R. Haensel *et al.* in Ref. 16; E. E. Koch *et al.* in Ref. 5; Schwenter *et al.* in Ref. 8; 0.17 eV by D. Pudewill *et al.* in Ref. 12; and 0.18 eV by E. Boursey *et al.* in Ref. 2).
[24]J. J. Fourney, A. Quattropani, and F. Bassani, Nuovo Cimento B 22, 153 (1974).
[25]A. Gold and R. S. Knox, Phys. Rev. 113, 834 (1959).
[26]For the general scheme of the calculation see F. Mueller, Phys. Rev. 153, 659 (1967).
[27]The value of $0.8m_e^*$ for the reduced mass of the exciton μ_{exc} has been already used by other authors (Ref. 13) as derived from their band calculations, and considering the effective mass of the hole infinite. In our band scheme, the effective mass of the conduction band at $\vec{k}=0$ turns out to be $m_e^*=0.878m_e$ in the $\vec{k}\cdot\vec{p}$ approach. Taking into account the finite value the effective mass of the hole (in the Δ direction $m_h^*=21m_e$ for the doubly-degenerate Δ_5 branch and $m_h^*=7m_e$ for the single lower branch Δ_1) we can take an average value of about $0.8m_e$ for μ_{exc}.
[28]E. U. Condon and G. H. Shortley, *The Theory of Atomic Spectra* (Cambridge U. P., London, 1967).
[29]J. Daniels and P. Krüger in Ref. 7; L. Schmidt in Ref. 7.